5-DOF control double stator motor for paediatric ventricular assist device

Masahiro Osa *
Ibaraki University
Ibaraki, Japan

Toru Masuzawa
Ibaraki University
Ibaraki, Japan

Eisuke Tatsumi
National cerebral and cardiovascular center
Osaka, Japan

Abstract

We have developed a maglev ventricular assist device (VAD) for use in infant patients, which requires the device to be smaller compared to adult devices. In this research, a miniaturized axial gap maglev motor for use as a paediatric VAD is reported. In addition, radial position control theory using P±2 pole algorithm is proposed, and the feasibility of radial position control with the miniaturized axial gap maglev motor is examined by using magnetic field analysis. The double stator motor consists of a top stator, a bottom stator and a levitated rotor set between the stators which have an identical structure. A double stator mechanism has been adopted to enhance motor torque with a smaller device size and a large air-gap. The rotational speed and the axial position of the rotor are regulated independently based on a vector control algorithm. The inclination and the radial position of the rotor are regulated using P±2 pole algorithm. The designed motor which has an outer diameter of 28 mm and total height of 41 mm can produce a radial force using P±2 pole algorithm, and indicates a possibility of 5 degrees of freedom (DOF) controlled axial gap double stator motor.

1 Introduction

Paediatric ventricular assist devices (VADs) require the device to be smaller in size and have better durability compared to adult devices. Additionally, it is necessary to regulate the blood flow by varying the rotational speed of the rotor over a wide operational range from 2000 RPM to 5000 RPM [1-2]. Active magnetic bearings, which can eliminate mechanical contacting components such as contact bearings and seals from the device, offer longer device lifetime and better blood compatibility of the blood pump [3]. Several axial double stator self-bearing motors, such as a combination of permanent magnets and a reluctance motors [4] or double permanent motors [5-6], have been developed. Self-bearing motors for use in paediatric VADs are required to be miniaturized, and have large air-gap, i.e., more than 1.5 mm, in order to avoid the blood damage due to high shear stress. The reluctance motor which does not have permanent magnets has disadvantage in terms of producing sufficient magnetic suspension forces and rotating torque with a smaller device size and large air-gap. The double permanent magnet motors require another passive or active magnetic bearing to support the radial direction or inclination of the rotor. We have developed a miniaturized 5-degrees of freedom (5-DOF) control axial gap type double stator maglev permanent magnet motor for use in paediatric VAD. The developed double permanent motor can be miniaturized and have large air-gap because the permanent magnet produce the high magnetic flux density in the air-gap. Furthermore the developed motor can actively control 5-DOF of the rotor without an additional passive or active magnetic bearing. In this paper, the double stator maglev motor is presented and the feasibility of radial position control of the rotor with the P±2 pole algorithm is examined.

2 Methods

2.1 Structure of 5-DOF control axial gap maglev motor

Figure 1 shows a schematic of the double stator maglev motor. The self-bearing motor consists of a top stator, a bottom stator and a levitated rotor set between the stators. Both stators have an identical structure and produce opposing forces it the axial direction. We have developed a double stator mechanism to enhance motor torque with a smaller device size and large air-gap. The top and bottom stators have two separate concentrated windings are set

*Contact Author Information: Toru MASUZAWA, masuzawa@mx.ibaraki.ac.jp, Department of Mechanical Engineering, Ibaraki University, 4-12-1, Nakanarusawa, Hitachi, Ibaraki, 316-8511, Japan, +81-294-38-5250, +81-294-38-5047

on each tooth. One of these windings controls the axial position and rotating speed of the rotor. The other winding controls the inclination and radial position of the rotor. The rotor includes permanent magnets on the both its surfaces facing the top and the bottom stators. The axial position and the rotating speed of the rotor are regulated independently using a vector control algorithm which can generate an axial attractive force and rotating torque with a single rotating magnetic field. The inclination and the radial position of the rotor are regulated by using P±2 pole algorithm.

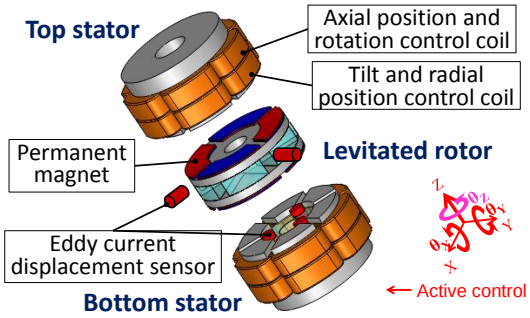

Figure 1: Basic structure of double stator maglev motor

2.2 Principle of axial position and rotation control

The axial force and the rotating torque will be regulated by changing the magnitude and the phase difference of the magnetic flux based on the vector control algorithm [7-8]. Three-phase currents are fed into the motor coils to produce an attractive force and rotating torque. Figure 2 shows the schematic of the vector control algorithm with double stator mechanism. The stator electromagnet and the permanent magnets of the rotor are assumed to produce sinusoidal magnetic fields which have peak flux density of B_e and B_p respectively. These magnetic fields have phase difference of ψ and pole pair number of M. The flux in the air-gap is generated in the axial direction, i.e. along the z-axis, and has constant values independently of the radial coordinate r.

$$B_E(\theta_Z, t) = B_e \cos(\omega t - M\theta_Z) \tag{1}$$

$$B_P(\theta_Z, t) = B_p \cos(\omega t - M\theta_Z - M\psi) \tag{2}$$

Where θ_Z is angler coordinate around z-axis and ω is rotating speed of the rotor. The coordinate axes are defined in Figure 2. A demagnetization curve of the permanent magnet is assumed to have a linear characteristic, and the load line of the permanent magnet has a linear relationship of flux density B_p in terms of coercivity of H_p .

$$B_p = \frac{B_r}{H_{cb}} H_p + B_r \tag{3}$$

$$B_p = \mu_0 \frac{l}{z} H_p \tag{4}$$

From these equations, the peak value of the flux density produced by the rotor permanent magnet can be calculated as follows.

$$B_p = \left(\frac{1}{B_r} + \frac{z}{l} \cdot \frac{1}{\mu_0 H_{cb}}\right)^{-1} \tag{5}$$

Where, the mean core length and the air-gap length between the rotor and the stator are defined as l and z. μ_0 is the permeability of the air-gap which is assumed to be same as a vacuum. The remanent flux density and the coercivity of the permanent magnet are described as B_r and H_{cb}.

For simplicity, magnetic properties inside the rotor and the stator are assumed to be homogenous and the reluctance of the core is ignored when compared with that of the air-gap. The peak value of the flux density produced by the electromagnet can be shown in terms of turn number of windings which defined as n and peak excitation current I_e to produce the flux density B_e.

$$B_e = \frac{\mu_0 n I_e}{z} \tag{6}$$

The magnetic stored energy, which is defined as W_g, can be expressed in terms of the energy density of the magnetic flux density integrated over the volume in the air-gap of the motor. Then the axial force F_z and rotating torque τ_z produced by a single stator can be expressed as follows [9-11],

$$F_z = \frac{\partial W_g}{\partial z} = \frac{(r_2^{\,2} - r_1^{\,2})\pi}{4\mu_0}\{B_p^{\,2} + 2B_p B_e \cos M\psi + B_e^{\,2}\} \tag{7}$$

$$\tau_z = \frac{\partial W_g}{\partial \psi} = \frac{zM(r_2^{\,2} - r_1^{\,2})\pi}{2\mu_0} B_p B_e \sin\psi \tag{8}$$

Where, r_1 and r_2 are the inner and outer radii of the rotor. To control the axial position and the torque of the rotor independently, the stator flux density B_e is divided into the direct axis component B_d and the quadrature axis component B_q corresponding to the flux components in the direction of the permanent magnets. B_d and B_q are defined as follows,

$$B_d = \sqrt{\tfrac{3}{2}} B_e \cos\psi = \sqrt{\tfrac{3}{2}} \frac{\mu_0 n I_e}{z} \cos\psi \tag{9}$$

$$B_q = \sqrt{\tfrac{3}{2}} B_e \sin\psi = \sqrt{\tfrac{3}{2}} \frac{\mu_0 n I_e}{z} \sin\psi \tag{10}$$

Where we assume that the magnetic flux of the d-axis produced by the top stator and bottom stator are B_{d1} and B_{d2}, and the magnetic flux of the q-axis produced by the top stator and bottom stator are B_{q1} and B_{q2}. The magnetic flux have the following relationship to produce the axial attractive force and the rotating torque independently.

$$B_{d1} = -B_{d2} = B_d \tag{11}$$

$$B_{q1} = B_{q2} = B_q \tag{12}$$

A resultant attractive force is produced as a differential of the attractive force between the top stator and the bottom stator. The rotating torque is produced as summation of the rotating torque between the top stator and the bottom stator [12-14].

$$F = \sqrt{\frac{2}{3}} \frac{(r_2^{\,2} - r_1^{\,2})\pi}{\mu_0} B_p B_d \tag{13}$$

$$\tau = \sqrt{\frac{2}{3}} \frac{zM(r_2^{\,2} - r_1^{\,2})\pi}{\mu_0} B_p B_q \tag{14}$$

From these equations, the motor and the attractive force is controlled with d-axis current and the rotating torque is controlled with q-axis current independently.

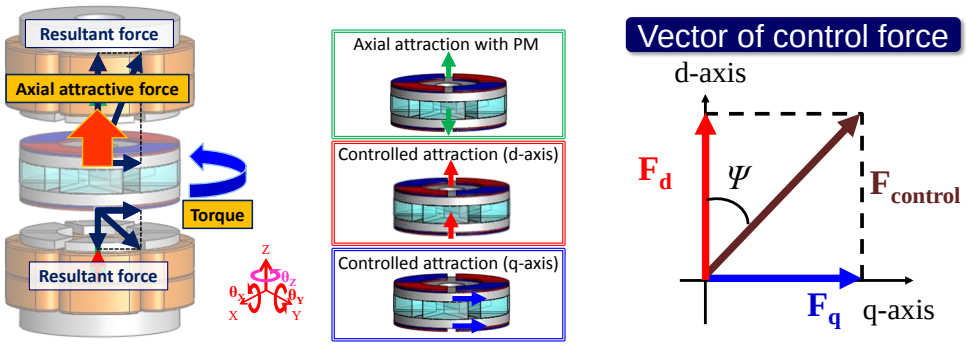

Figure 2: Principle of vector control

2.3 principle of tilt control

The inclination of the rotor can be regulated by using P±2 pole algorithm. Figure 3 shows the schematic of the P± 2 pole algorithm. The stator electro magnet is assumed to produce two sinusoidal rotating magnetic fields which have peak flux density of *Btx*, *Bty* and have a phase difference of 90 degrees among each other to control the inclination around x-axis and y-axis. These flux densities have pole pair number of *N*.

$$B_T(\theta_Z, t) = B_{tx}\sin(\omega t - N\theta_Z) + B_{ty}\cos(\omega t - N\theta_Z) \tag{15}$$

A total magnetic flux density B_g in the air-gap will be determined as a summation of the flux densities B_p and B_T. A restoring torque act on a minute area of the rotor surface is expressed as follow.

$$\Delta\tau(\theta) = \frac{{B_g}^2}{2\mu_0}\Delta S \tag{16}$$

A total restoring torque can be generated by an imbalance of the magnetic flux distribution. The restoring torque is calculated as the integration of Equation (16) in terms of radial coordinate *r* and angler coordinate θ.

$$T = \int_0^{2\pi}\int_{r_1}^{r_2}\Delta\tau\, dr d\theta \tag{17}$$

The restoring torque can be divided into two restoring torques around x-axis and y-axis.

$$T = T_x + T_y = \int_0^{2\pi}\int_{r_1}^{r_2}\Delta\tau\sin\theta dr d\theta + \int_0^{2\pi}\int_{r_1}^{r_2}\Delta\tau\cos\theta dr d\theta \tag{18}$$

Constant restoring torques around x-axis and y-axis can be generated when $M–N = \pm 1$.

$$T_x = \frac{B_p B_{tx}(r_2 - r_1)}{4\mu_0}\int_0^{2\pi}\{\cos(M-N-1)\theta - \cos(M-N+1)\theta\}d\theta = \frac{B_p B_{tx}(r_2 - r_1)\pi}{2\mu_0} \tag{19}$$

$$T_y = \frac{B_p B_{tx}(r_2 - r_1)}{4\mu_0}\int_0^{2\pi}\{\cos(M-N-1)\theta - \cos(M-N+1)\theta\}d\theta = \frac{B_p B_{tx}(r_2 - r_1)\pi}{2\mu_0} \tag{20}$$

Figure 4 shows a relationship between an arrangement of magnetic fields based on P±2 pole algorithm and the resulting restoring torque. Where, the stator pole is assumed to be positioned above the rotor pole.

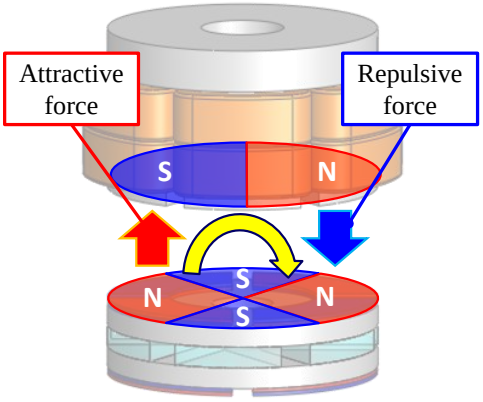

Figure 3: Principle of tilt control

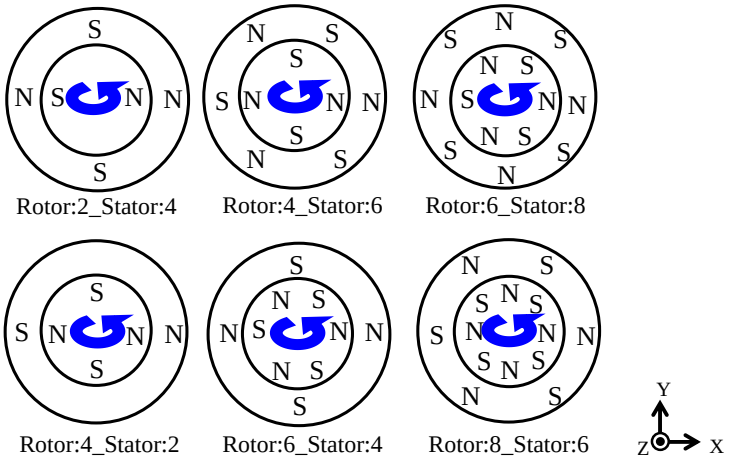

Figure 4: Restoring torque production theory

2.4 Principle of radial force control

We have found a radial force can be generated using P±2 pole algorithm. A rotor radial position control method utilizing the radial force was developed. Figure 5 shows a principle of radial force production using P±2 pole algorithm. For simplicity a motor which has four pole rotor magnets is considered. The electromagnet produces a two pole magnetic field. The interaction between the two fields produced by the permanent magnets and the electromagnet generate attraction and repulsion forces which contain components in the radial direction. As a result, a magnetic force can be generated in the radial direction of the motor. The radial force can be generated in the x direction when the restoring torque is produced around y-axis. On the other hand, the radial force in y direction can be produced by stator field to control an inclination around x-axis. Figure 6 shows a relationship between an arrangement of magnetic fields based on P±2 pole algorithm and a direction of the radial force. Where, the stator pole is assumed to be positioned above the rotor pole.

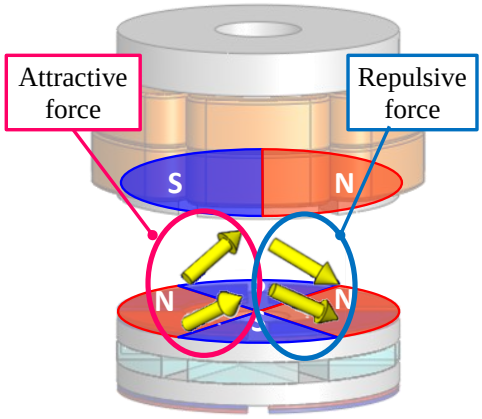

Figure 5: Principle of radial position control

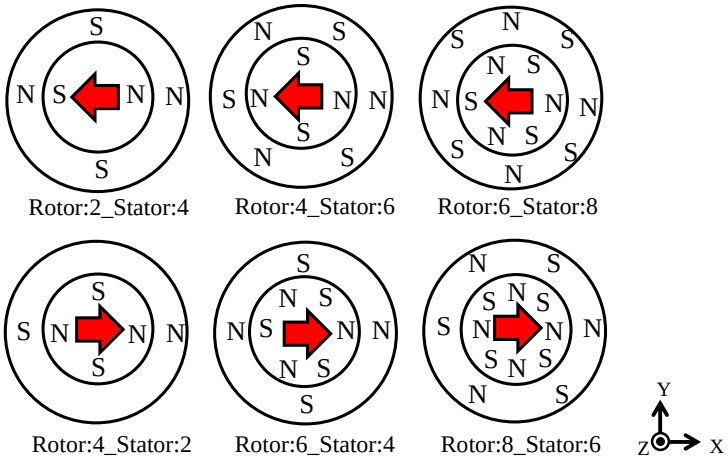

Figure.6: Radial force production theory

2.5 Independency of tilt control and radial position control

The restoring torque and the radial force can be produced independently with the double stator mechanism. Figure 7 shows the principles of the tilt control around y-axis and the radial position control in x direction of the rotor. As shown in Figure 7(a), when the top and the bottom stators produce the restoring torque in the same direction, the radial forces produced by the top stator and the bottom stator cancel each other. Therefore the motor can generate a restoring torque. In case that a restoring torque produced by the top stator and the bottom stator are regulated in an opposite direction, the motor can generate a radial force as shown in Figure 7(b). Consequently, the inclination and the radial position of the rotor can be controlled by regulating the magnitude and the direction of excitation currents fed into the top stator and the bottom stator.

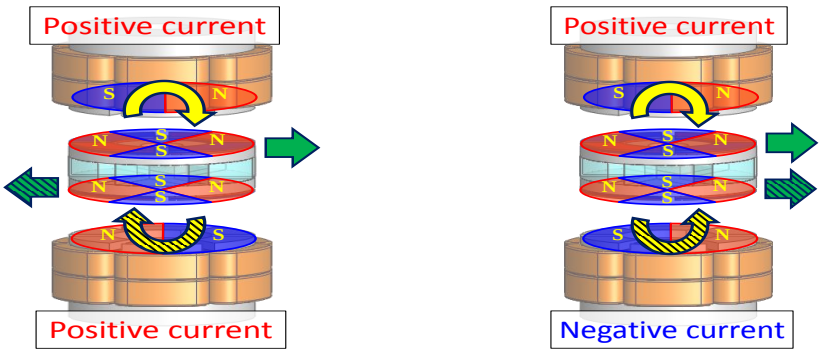

(a) Inclination control (b) Radial position control

Figure 7: Principle of restoring torque and radial force control

2.6 Three dimensional magnetic field analysis

Three dimensional magnetic field analysis has been performed to confirm the principle of the restoring torque and the radial force production using P±2 pole algorithm. The restoring torque and the radial force have been evaluated by changing a combination of the pole number among a rotor and a stator. The rotational angle of the rotor is changed in increments of 30 degrees of electrical angle. Pole numbers of the rotor fields and the stator fields are defined as P and E respectively. The combinations of the pole number, i.e. P:E, are determined as 2:4, 4:2, 4:6, 6:4, 6:8, 8:6. A core material of the rotor and the stator is magnetic steel iron (SUY-1) and has B-H characteristics shown in Figure 8. The material of the permanent magnets is Nd-Fe-B which has a coercivity of 907 kA/m and residual flux density of 1.36 T. The restoring torque is produced around the y-axis and the radial force is produced in the x direction.

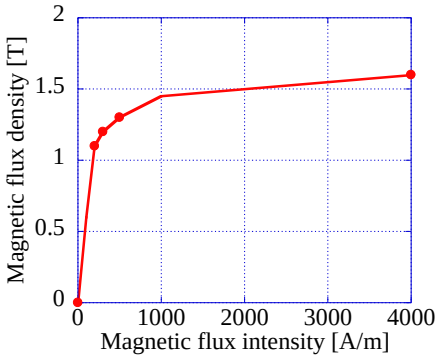

Figure 8: B-H characteristics of core material

2.6.1 Confirmation of restoring torque and radial force production theory

In this section, an initial estimate of the restoring torque and the radial force production were determined using permanent magnets and magnetic steel irons. The stator slots were removed from the simulation geometry and the stator magnetic field was simulated using permanent magnets. The permanent magnets have thickness of 0.7 mm are set on the rotor and the stator surfaces based on the proposed P±2 pole algorithm. Figure 9 shows a schematic of a simulation geometry model and Figure 10 shows four arrangement pattern of permanent magnets at a rotating angle of 0 degree. A diameter of the model is 26 mm, and air gap length is 1.5 mm.

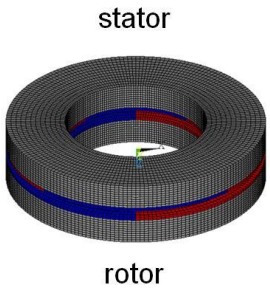

Figure 9: Simulation geometry

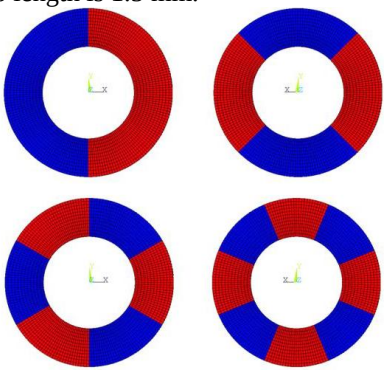

Figure 10: Pole arrangement of the permanent magnets

2.6.2 Evaluation of the relationship between pole combination and restoring torque and radial force

A 5-DOF controlled maglev motor for use in paediatric VAD was designed to determine the feasibility of an inclination and a radial position control rotor. The designed motor consists of single stator to simplify the simulation model. Figure 11 shows a schematic of the simulation model. The stator has 12 slots and concentrated winding coils which have turn number of 50 turns are wound on each tooth. Stator fields are produced by the excitation of the electromagnetic windings. Permanent magnets have a thickness of 0.7 mm, and have the same configuration as shown in Figure 10. The stator and the rotor have outer diameter of 28 mm, total height of the motor is 19.7 mm. An air gap length is 1.5 mm.

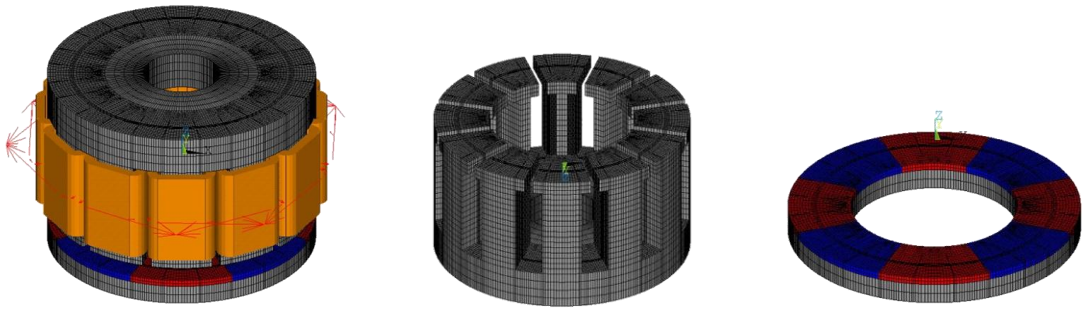

Figure 11: Analytical model of 12 slots axial gap maglev motor

3 Results

3.1 Confirmation of restoring torque and radial force production theory

Figure 12 shows the relationship between the electrical rotating angle of the rotor and restoring torque. Figure 13 shows a relationship between the combination of the pole number and an averaged restoring. The restoring torque oscillated according to the electrical rotational angle, and the amplitude became larger with combinations with a smaller pole number. The averaged restoring torque that could be generated was almost constant, independent of the combination of the pole number with the exception of combinations with P=2 with E=4 or P=4 with E=2.

Figure 14 shows a relationship between the electrical rotational angle of the rotor and absolute value of radial force. Figure 15 shows the relationship between the combinations of the pole number. Similar to the result of restoring torque, the radial force fluctuated according to the electrical rotational angle. The averaged radial force increased as the smallest pole number of either P or E increased.

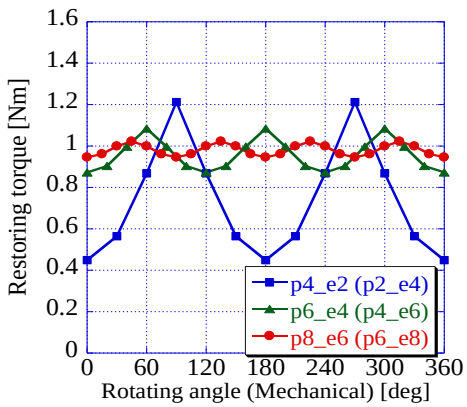

Figure 12: Rotating angle and restoring characteristics

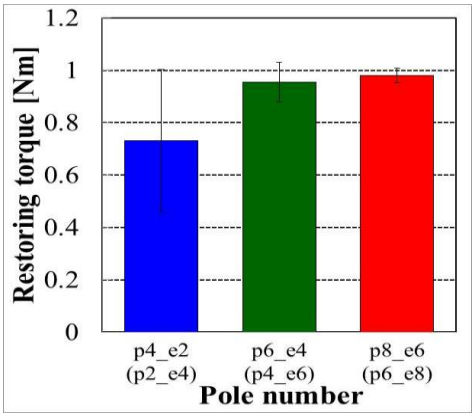

Figure 13: Pole number and restoring characteristics

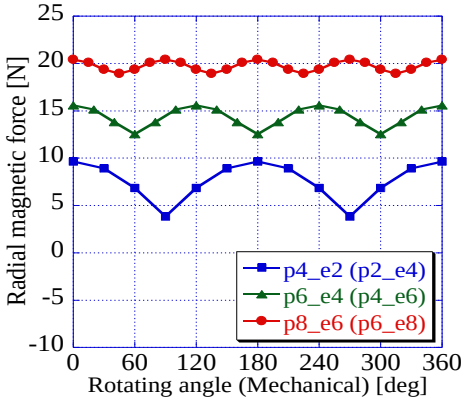

Figure 14: Rotational angle and radial force characteristics

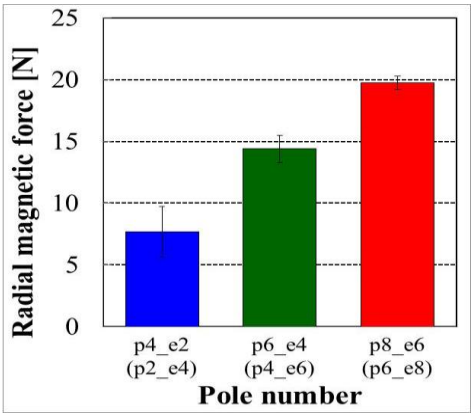

Figure 15: Pole number and radial force characteristics

Figure 16 shows a flux density distribution of the rotor and stator core. The magnetic saturation area at the rotor and stator core with pole combinations of P=2 with E=4 (or P=4 with E=2), was larger than the core with other combinations.

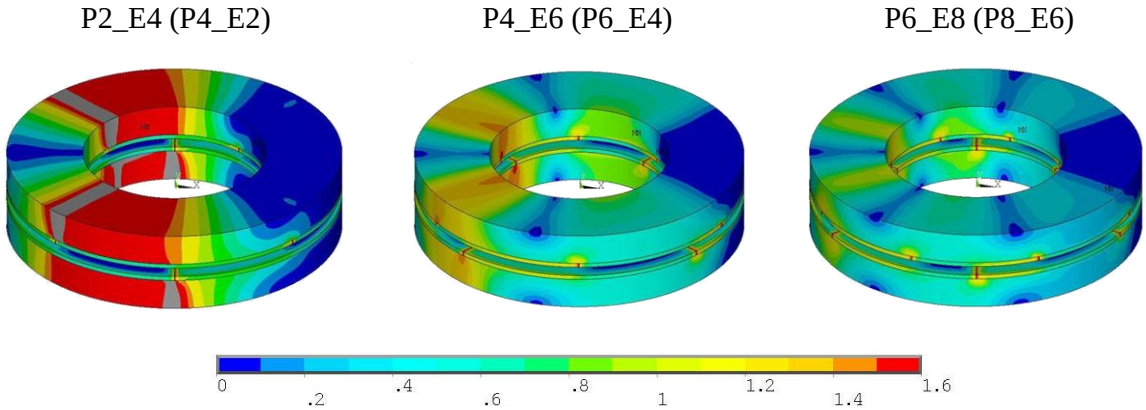

Figure 16: Magnetic flux distribution of the core material

3.2 Evaluation of restoring torque and radial force

Figure 17 and Figure 18 show a relationship between the combination of pole numbers and an averaged restoring torque, and an averaged radial force. The radial force generated in a negative direction is marked with an asterisk in Figure 17. The restoring torque and the radial force produced by the motor tended to become larger in the case of the stator pole number of E=P+2. In particular the motor which has the rotor pole number of 6 and stator pole number of 8 could produce a maximum restoring torque of 14 mNm/A and a maximum radial force of 0.64 N/A respectively. In addition, the radial force produced by the motor increased according to an increase of a motor pole number.

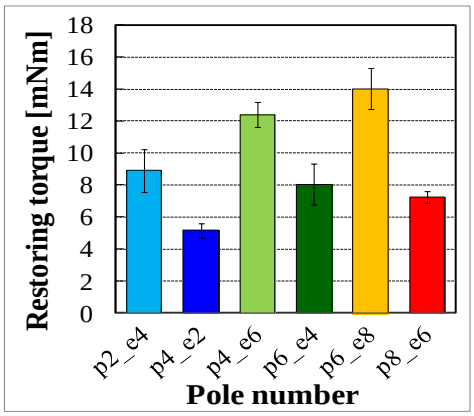

Figure 17: Pole number and restoring characteristics

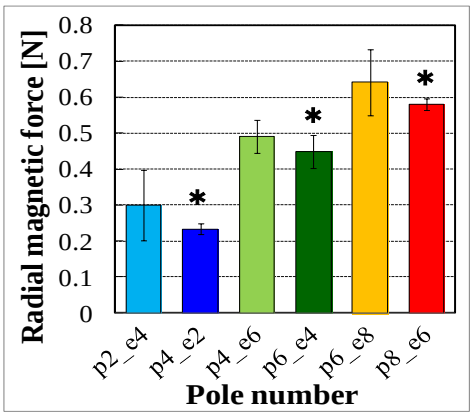

Figure 18: Pole number and radial force characteristics

4 Discussion

The magnetic fields produced by the rotor permanent magnets and stator electromagnets based on P±2 pole algorithm can produce the constant restoring torque and radial force independently of the rotational angle of the rotor. The double stator structure is a strong candidate to control the 5-DOF of the rotor based on vector control algorithm and P±2 pole algorithm with a miniaturized axial gap maglev motor.

The restoring torque and the radial force fluctuate against the change of the rotational angle of the rotor as shown in Figure 12 and Figure 14, and this amplitude become smaller with the larger pole number. The fluctuation is caused due to the harmonics of the flux density in the air-gap. Increasing the pole number of the motor is

effective to eliminate the harmonics, and can suppress the fluctuation caused by the change of rotational angle of the rotor.

As shown in Figure 13, the restoring torque tends to be small as the rotor pole number P=2 and stator pole number E=4 (or P=4, E=2) compare to the models which have other combinations of the pole number. This is because the magnetic saturation area in the rotor and stator core become larger if when the pole number is small.

The radial force can be increased according to the increase of pole number of the motor as shown in Figure 15 and Figure 18. The radial force has a similar relationship as the rotating torque and pole number of the motor. Therefore, the relationship between the radial force and the torque around the z-axis produced by the magnetic field based on P±2 pole algorithm should be confirm in a future study.

A larger restoring torque and radial force produced by the motor can be obtained with a combination of the stator pole number of E=P+2 as shown in Figure 17 and Figure 18. This phenomenon could be due to the geometry of the motor stator and magnetic field produced by the stator electromagnets, as this phenomenon was not observed with the simulation model that did not have any slots.

5 Conclusion

A double stator axially levitated motor for paediatric VAD and radial position control method by using P±2 pole algorithm has been proposed. The proposed motor actively control 5-DOF of the rotor by using vector control algorithm and P±2 pole algorithm. The radial force production can be confirmed from analytical results. This device shows it is possible to achieve a smaller device size and the analytical results have demonstrated the feasibility of 5-DOF control of the rotor with axial gap double stator motor.

References

[1] J. Timothy Baldwin, Harvey S. Borovets, Brian W. Duncan, Mark J. Gartner, Robert K. Jarvik, William J. Weiss and Tracey R. Hoke, The National Heart, Lung, and Blood Institute Pediatric Circulatory Support, Journal of the American heart association, pp.147-155, 2006.

[2] Brian W. Duncan, Mechanical circulatory support for infants and children with cardiac disease, The Annals of Thoracic Surgery, 73, pp.1670-1677, 2002.

[3] Onuma H, Murakami M and Masuzawa T, Novel Maglev pump with a combined magnetic bearing, ASAIO Journal, 51(1), pp.50-55, 2005.

[4] Akira Chiba, Tadashi Fukao, Osamu Ichikawa, Masahide Oshima, Masatsugu Takemoto, David G.Dorrell, Magnetic Bearings and Bearingless Drives, Newnes, pp.318-328, 2005.

[5] Satoshi Ueno, Toshiyuki Okamura, Masaaki Sakagami, Shigeo Tanaka, Development of Miniaturized Regenerative Pump using Axial Self-Bearing Motor, The 12th ISMB, pp.180-188, 2010.

[6] Tatsushi Suzuki, Satoshi Ueno, Tsunehiro Takeda, Development of a Vacuum Pump usin Axial-Gap Self-Bearing Motor and Superconducting Magnetic Bearing, The 12th ISMB, pp.733-741, 2010.

[7] Masuzawa T, Ezoe S, Kato T, Okada Y, Magnetically suspended centrifugal blood pump with an axially levitated motor, Artificial Organs, 27, 10, pp.631-638, 2003.

[8] Masahiro Osa, Toru Masuzawa, Eisuke Tatsumi, Miniaturized axial gap maglev motor with vector control for pediatric artificial heart, The 20th MAGDA Conference in Pacific Asia, 2A11,2011

[9] Kato T, Masuzawa T, Ezoe S, Magnetically levitated rotary artificial heart with axial suspension motor, The 8th ISMB, pp.9-14, 2002.

[10] Nicholas A. Greatrex, Daniel L. Timms, Edward W. Palmer, Toru Masuzawa, Axial magnetic bearing development for the BiVACOR Rotary BiVAD/TAH, IEEE Transactions on Biomedical Engineering, 57, 3, pp.714-721, 2010.

[11] Nobuyuki Kurita, Daniel L Timms, Nicholas Greatrex, Toru Masuzawa, Axial magnetic bearing development for the BIVACOR roary BiBAD/TAH, The 11th ISMB, pp.217-224,2008.

[12] Satoshi Ueno, Yohji Okada, Characteristics and control of a bidirectional axial gap combined motor-bearing, IEEE, Asme Transactions on Mechatronics,5,3,pp.310-318, 2000.

[13] Yoji Okada, Naoto Yamashiro, Kunihiro Ohmori, Toru Masuzawa, Mixed flow artificial heart pump with axial self-bearing motor, IEEE/ASME Transactions on Mechatronics, 10, pp.658-665, 2005.

[14] Quang Dich Nguyen, Nobukazu Shimai, Satoshi Ueno, Control of 6 Degrees of Freedom Salient Axial-Gap Self Bearing Motor, The 12th ISMB, pp.627-634, 2010.